

Quaternary alloy $\text{Zn}_{1-x}\text{Mg}_x\text{S}_y\text{Se}_{1-y}$

Hiroyuki Okuyama, Yuko Kishita, and Akira Ishibashi

Sony Corporation Research Center, Fujitsuka 174, Hodogaya, Yokohama 240, Japan

(Received 29 September 1997)

The band-gap energy of II-VI compound semiconductors was simply calculated using a modified dielectric theory. The calculated band-gap energies of MgS and MgSe were 4.62 and 3.67 eV. From the extrapolation of the band-gap energies of $\text{Zn}_{1-x}\text{Mg}_x\text{Se}$ and $\text{Zn}_{1-x}\text{Mg}_x\text{S}$, the band-gap energies of MgSe and MgS of zinc blende at room temperature were determined to be 3.59 and 4.45 ± 0.2 eV, almost the same as the value calculated using the modified dielectric theory. The bowing parameter of the $\text{Zn}_{1-x}\text{Mg}_x\text{Se}$ ternary alloy was experimentally obtained as 0 eV, which can be explained in terms of the modified dielectric theory. The lattice constant of the quaternary alloy $\text{Zn}_{1-x}\text{Mg}_x\text{S}_y\text{Se}_{1-y}$ can be expressed by Vegard's law [Z. Phys. **5**, 17 (1921)]. The band-gap energy of $\text{Zn}_{1-x}\text{Mg}_x\text{S}_y\text{Se}_{1-y}$ can be expressed by the parabolic function of the composition considering the bowing parameter, where we use of 4.65, 3.59, 3.68, and 2.69 eV as the band-gap energies of MgS, MgSe, ZnS, and ZnSe, respectively. [S0163-1829(98)10303-X]

I. INTRODUCTION

In fabricating semiconductor devices, it is important to know the band parameters such as the band-gap energy. Methods of calculating the band parameters from empirical parameters have been developed and applied to semiconductor devices. First, the band structure was calculated using the pseudopotential theory reported by Phillips in 1958.¹ In 1969 Van Vechten proposed the dielectric theory.²⁻⁴ Stringfellow calculated the band-gap energy of III-V compounds using the dielectric theory and found the calculated results consistent with the experimental results.⁵ However, the band-gap energy of some II-VI compounds had not been experimentally obtained until recently because it was difficult to grow high-quality crystals due to the high ionicity of these compounds. Thus this dielectric theory has not been applied to II-VI compounds.

The II-VI compound laser diodes (LD's) have undergone rapid development in the past few years. In 1996, Taniguchi *et al.* reported a long-life II-VI laser diode.⁶ The device lifetime under room temperature (RT) continuous-wave (CW) operation was more than 100 h. It is expected that the device lifetime of II-VI laser diodes will become comparable to that of III-V LD's such as $\text{Al}_x\text{Ga}_{1-x}\text{As}$ LD's. In II-VI laser diodes, it is necessary to use $\text{Zn}_{1-x}\text{Mg}_x\text{S}_y\text{Se}_{1-y}$ as the cladding layer^{7,8} in order to achieve RT CW operation.⁹ $\text{Zn}_{1-x}\text{Mg}_x\text{S}_y\text{Se}_{1-y}$ is one of the most popular materials among II-VI compound semiconductors now. It is important to obtain the band parameters of $\text{Zn}_{1-x}\text{Mg}_x\text{S}_y\text{Se}_{1-y}$ in order to improve the II-VI laser diodes.

Band parameters such as the band-gap energy and the bowing parameter and crystal structures in II-VI compound semiconductors such as $\text{Zn}_{1-x}\text{Mg}_x\text{S}_y\text{Se}_{1-y}$ are discussed in this paper. We calculated the band-gap energy and lattice constants of all II-VI compound semiconductors and compared the calculated values to the experimental values. To calculate the band-gap energy we modified the dielectric theory of Van Vechten so that it could be applied to II-VI compounds whose crystal structure is zinc blende. Although the crystal structure of MgS and MgSe is reported to be

wurtzite or rocksalt,¹⁰ the structure becomes a zinc-blende structure in quaternary $\text{Zn}_{1-x}\text{Mg}_x\text{S}_y\text{Se}_{1-y}$. The band-gap energy of zinc-blende MgS and MgSe must be known to calculate the band-gap energy of this quaternary alloy. Although the properties of the III-V alloys were studied by Adachi¹¹ and Williams *et al.*,¹² there are few papers on the properties of II-VI alloys. We therefore calculated the properties of the $\text{Zn}_{1-x}\text{Mg}_x\text{S}_y\text{Se}_{1-y}$ quaternary alloy.

II. ESTIMATE OF LATTICE CONSTANT

The lattice constants of compounds can be obtained from the covalent radii and the ionic radii. The lattice constant a_{ZB} of a binary compound AB whose crystal structure is a zinc blende can be obtained using the following equation from the sum of the tetrahedral covalent radii¹³ (r_{covalent}) of cation A and anion B , which are shown in Table I:

$$a_{\text{ZB}} = 4\sqrt{3}(r_{\text{covalent}}^A + r_{\text{covalent}}^B). \quad (1)$$

Table II shows various a_{ZB} calculated using Eq. (1) and Table I. The lattice constant of a rocksalt structure a_{rocksalt} is expressed by the sum of the ionic radii (r_{ionic}) in Table I as

$$a_{\text{rocksalt}} = 2(r_{\text{ionic}}^A + r_{\text{ionic}}^B). \quad (2)$$

Table I also shows the electronegativity (X) and half of the sum of the ionization energy (I) and the electron affinity (A) of various elements. We can see the following tendencies in Table I.

(i) The covalent radius r_{covalent} decreases as the atomic number increases on the same row. This shows that the average radius of the outermost orbital (the outermost orbital being the orbital with the outermost electron) becomes smaller as the nuclear charge increases. Even when the azimuthal quantum number increases, the shrinkage of the average radius of the orbital is more pronounced than the expansion by the additional orbital in the same row.

(ii) In the same column, the tetrahedral covalent radius increases as the row number increases except for Ga, Al, Zn, and Mg. This means that the degree of shrinkage of the av-

TABLE I. Tetrahedral covalent radii (r_{covalent}), ionic radii (r_{ionic}), electronegativity (X), and half of the sum of the ionization energy and the electron affinity [$(I+A)/2$] (Refs. 13, 16, 17, and 23).

Column	I	II	III	IV	V	VI	VII	VIII
row II	Li	Be	B	C	N	O	F	Ne
ionic radius (nm)	0.068	0.035	0.023	0.015	0.171	0.140	0.136	0.158
covalent radius (nm)		0.106	0.088	0.077	0.070	0.066	0.064	
electronegativity	1	1.5	2	2.5	3	3.5	4	
$(I+A)/2$ (eV)	3.00	4.36	4.29	6.26	7.23	7.54	10.41	
row III	Na	Mg	Al	Si	P	S	Cl	Ar
ionic radius (nm)	0.097	0.065	0.050	0.041	0.212	0.184	0.181	0.188
covalent radius (nm)		0.140	0.126	0.117	0.110	0.104	0.099	
electronegativity	0.9	1.2	1.5	1.8	2.1	2.5	3	
$(I+A)/2$ (eV)	2.84	3.37	3.21	4.77	5.62	6.22	8.29	
row IV	Cu	Zn	Ga	Ge	As	Se	Br	Kr
ionic radius (nm)		0.074	0.062	0.053	0.222	0.198	0.195	0.200
covalent radius (nm)	0.135	0.131	0.126	0.122	0.118	0.114	0.111	
electronegativity	1.9	1.6	1.6	1.8	2	2.4	2.8	
$(I+A)/2$ (eV)	4.48	4.70	3.15	4.55	5.31	5.89	7.59	
row V	Ag	Cd	In	Sn	Sb	Te	I	Xe
ionic radius (nm)	0.126	0.097	0.081	0.071	0.245	0.221	0.216	0.217
covalent radius (nm)	0.152	0.148	0.144	0.140	0.136	0.132	0.128	
electronegativity	1.9	1.7	1.7	1.8	1.9	2.1	2.5	
$(I+A)/2$ (eV)	4.44	4.50	3.04	4.27	4.86	5.49	6.75	

TABLE II. Calculated (Calc.) and experimental (Expt.) values of the lattice constants a (Å) and E_0 (eV). ΔX is the difference in electronegativity between a cation and an anion. D is a parameter that shows the effect of the d electron. Calculated values were obtained using Eqs. (1) and (6). The experimental values were obtained from Refs. 20, 24, and 25 and this experiment.

Material	ΔX	D	a (Calc.)	a (Expt.)	E_0 (Calc.)	E_0 (Expt.)
MgS	1.3	1.00	5.635	5.620	4.62	4.45±0.2
MgSe	1.2	1.07	5.866	5.890	3.67	3.59
MgTe	0.9	1.07	6.282	6.280	3.01	2.90
ZnS	0.9	1.07	5.427	5.409	3.72	3.68
ZnSe	0.8	1.16	5.658	5.668	2.62	2.69
ZnTe	0.5	1.16	6.074	6.103	2.10	2.26
CdS	0.8	1.16	5.820	5.832	2.56	2.42
CdSe	0.7	1.26	6.051	6.050	1.85	1.70
CdTe	0.4	1.27	6.466	6.479	1.39	1.56
Si	0	1.00	5.404	5.431	4.10	4.10
Ge	0	1.25	5.635	5.646	1.02	0.90
Sn	0	1.46	6.466	6.489	0.08	-0.40
AlP	0.6	1.00	5.450	5.451	4.23	3.58
AlAs	0.5	1.11	5.635	5.661	2.75	3.02
AlSb	0.4	1.17	6.051	6.136	1.92	2.22
GaP	0.5	1.11	5.450	5.451	2.90	2.75
GaAs	0.4	1.23	5.635	5.653	1.52	1.42
GaSb	0.3	1.31	6.051	6.096	1.00	0.73
InP	0.4	1.20	5.866	5.869	1.81	1.35
InAs	0.3	1.33	6.051	6.058	0.87	0.36
InSb	0.2	1.42	6.466	6.479	0.54	0.17

erage radius of the outermost orbital caused by the increase of the nuclear charge is less than the degree of enlargement of the average radius of the outermost orbital caused by the addition of the new orbital due to the increase of the principal quantum number in the same column.

(iii) In group III, the tetrahedral covalent radii of Al and Ga are the same.

(iv) In group II, the tetrahedral covalent radius of Mg is larger than that of Zn. This is an exception to tendency (ii). This means that shrinkage of the average radius of the outermost orbital caused by the increase of the nuclear charge (12 for Mg to 30 for Zn) is more pronounced than the enlargement of the average radius of the outermost orbital ($3s, 3p$ for Mg to $4s, 4p$ for Zn) with the increase of the principal quantum number. There is no such tendency in the ionic radius.

Next we discuss the possibility of lattice matching between GaAs and $Zn_{1-x}Mg_xS_ySe_{1-y}$. Because Ga, As, Zn, and Se exist in the same row in the Periodic Table, the lattice constants of these compounds are almost the same. For ZnS_ySe_{1-y} to be lattice matched to GaAs, y must be 0.07, while $Zn_{1-x}Mg_xS_ySe_{1-y}$ has two parameters, x and y , and its band parameters such as the band-gap energy can be varied while maintaining the lattice match to GaAs.⁸ This is due to tendency (iv) for the covalent radius of Zn to be smaller than that of Mg.

When ternary alloy $A_xB_{1-x}C$ is fabricated, the lattice constant $a(A_xB_{1-x}C)$ is expressed by the linear combination of the lattice constants between binary compound AC and BC (a^{AC} and a^{BC}), the so-called Vegard law¹⁴

$$a(A_xB_{1-x}C) = xa^{AC} + (1-x)a^{BC}. \quad (3)$$

Because the lattice constants of all uniform semiconductor alloys studied up to this point can be, without exception, expressed by Vegard's law, the crystal structure of an alloy whose lattice constant is expressed by Vegard's law can be considered to be uniform and the crystal structure of the alloy the same as that of binary compounds. Let us now consider that if Vegard's law does not apply, the alloy may have a crystal structure different from binary compounds.

III. MODIFIED DIELECTRIC THEORY OF BAND-GAP ENERGY

One of the purposes of this paper is to calculate the band-gap energy of II-VI compound semiconductors using the lattice constant, electronegativity, and atomic number. From Phillips's pseudopotential theory, the band-gap energy E_g is expressed by¹⁻³

$$E_g = (E_h^2 + C^2)^{1/2}, \quad (4)$$

where E_h is the homopolar band-gap energy and C is the heteropolar band-gap energy. From the dielectric theory, the difference in energy between the conduction-band minimum and the valence-band maximum at the Γ point (E_0) is expressed by the following equation when the influence of the d electron is included:^{2,3}

$$E_0 = [E_h - (D-1)\Delta E_0][1 + (C/E_h)^2]^{1/2}, \quad (5)$$

where D is a term reflecting the influence of d electrons on the band gap and ΔE_0 and E_h are functions only of lattice constant a . C can be estimated from the experimental value of the dielectric constant and is almost proportional to the difference in electronegativity (ΔX^{AB}) between A and B of the binary compound AB .^{2,3} However, we found that the dielectric theory cannot be applied to II-VI compound semiconductors as is. So we modified the theory to express the band-gap energy of II-VI compounds.

In our modified dielectric theory, a parameter expressing the d -electron effect is added to the homopolar band-gap energy in Eq. (4) because the energy of the s orbital, which penetrates the d band, decreases considerably when d electrons exist. Therefore, the band-gap energy E_0 can be expressed by

$$E_0 = \{[E_{h0} - (D-1)\Delta E_0]^2 + C_0^2\}^{1/2}, \quad (6)$$

$$E_{h0} = 4.1(a/a_{Si})^{-2.75} \quad (\text{eV}), \quad (7)$$

$$\Delta E_0 = 12.8(a/a_{Si})^{-5.07} \quad (\text{eV}), \quad (8)$$

$$C_0 = k_C \Delta X^{AB} \quad (\text{eV}), \quad (9)$$

where E_{h0} is the homopolar band-gap energy and C_0 is the heteropolar band-gap energy in the modified dielectric theory. D is a term reflecting the influence of d electrons on the homopolar band gap. E_{h0} and ΔE_0 are functions of lattice constant a . a_{Si} is the lattice constant of Si. Equations (7) and (8) are experimentally derived from the band-gap energy of group-IV semiconductors with no heteropolar band gap such as C, Si, Ge, and Sn and are the same equations that Van Vechten used.^{2,3} In Van Vechten's theory, C_0 is proportional to the difference of the electronegativity between cation A and anion B in Table I. We define this proportional coefficient as k_C . The electronegativity defined by Pauling¹³ (X) is almost the same as that defined by Mulliken.¹⁵ The electronegativity defined by Mulliken is expressed by half of the sum of the ionization energy¹⁶ [I (eV)] and the electron affinity¹⁷ [A (eV)], which is shown in Table I. Therefore, in group-II and -VI elements, the following relation can be obtained:

$$(I^B + A^B)/2 - (I^A + A^A)/2 = 2.1\Delta X^{AB} \quad (\text{eV}). \quad (10)$$

If the arbitrary unit Pauling uses to express electronegativity is transformed into the eV Mulliken uses to express electronegativity, the proportional coefficient becomes 2.1. If we assume that C_0 is equal to the left-hand side of Eq. (10), we can determine that k_C is 2.1. The experimental value is almost the same as the calculated value if we make this assumption.

The D parameter of a compound AB composed of cation A and anion B is expressed by the empirical equation²

$$D(A, B) = \Delta^A \Delta^B - (\delta^A \delta^B - 1)(Z^A - Z^B)^2, \quad (11)$$

where Z^A (Z^B) is the number of valence electrons of cation A (anion B) and Δ^A (Δ^B) is the parameter of cation A (anion B) that depends on the row number. In addition, if the row number is the same, $\Delta^A = \Delta^B$. When AB is a group-IV semiconductor and $Z^A - Z^B = 0$, it is easily understood that $\Delta^A = \Delta^B = D^{1/2}$. So Δ can be obtained from the D of group-IV

TABLE III. Δ and δ as a function of the row number.

Row	$\Delta_{(\text{cation})}$	$\Delta_{(\text{anion})}$	$\delta_{(\text{cation})}$	$\delta_{(\text{anion})}$
II	1	1	1.000	1.000
III	1	1	1.000	1.000
IV	1.12	1.12	1.003	1.003
V	1.21	1.21	<u>1.003</u>	<u>1.009</u>

semiconductors such as Ge and Sn. These parameters are summarized in Table III. δ^A (δ^B) is the parameter of the cation (anion), which becomes more important as $(Z^A - Z^B)^2$ becomes larger. δ^A and δ^B are functions of the row number. At rows II and III, $D=1$ because there is no d electron. At rows IV and V, we modified the values of δ^A and δ^B because $Z^A - Z^B$ of II-VI compound semiconductors is twice of that of III-V compound semiconductors and the contribution of δ^A and δ^B becomes larger, as the modified theory can be applied to II-VI compound semiconductors such as CdSe and ZnTe with large D . So we use these four values of δ^A and δ^B (underlined in Table III) in our modified theory. Although in Ref. 2 δ^A and δ^B are the same on the same row, we propose that δ^A is different from δ^B even on the same row for the following two reasons.

(i) In a compound semiconductor, the conduction band is formed from the antibonding states of the s orbital of the cations and the valence band is formed from the bonding state of the p orbital of the anions. These facts suggest that the effect of the d electron of the cation is larger than that of the anion because the energy of the s orbital, which penetrates the d band, is reduced more by the effect of the d electron than that of the p orbital.

(ii) The d electron has various energy levels. For example, the binding energy of both Zn $3d$ and Cd $4d$ is 9 eV and the binding energies of Se $3d$ and Te $4d$ are 57 eV and 40 eV, respectively.¹⁸ It is obvious that the effect of the d electron of a cation is different from that of an anion.

Next we calculated band-gap energy E_0 using our modified dielectric theory. Table II shows calculated E_0 and the experimental value of E_0 of various semiconductors. We used only four adjusting parameters and calculated E_0 of 18 materials as quite close to the experimental values. The calculated E_0 of zinc-blende MgS and MgSe are shown in Table II. From Eqs. (6)–(9) we can see that the main influences on the band-gap energy are the bond length between the cation and anion (the lattice constant), the difference of electronegativity between the cation and anion, and the effect of the d electron of both the cation and anion determined by the row number. These influences are reflected in the reason that E_0 of MgS is larger than that of ZnSe in spite of their having almost the same lattice constants being that there is no d -electron effect in MgS and that the difference in electronegativity between Mg and S is larger than that between Zn and Se. These influences are also reflected in the reason that E_0 of CdSe (1.70 eV) is different from that of ZnTe (2.26 eV) being that D of CdSe is different from D of ZnTe, although the lattice constants and the electronegativity differences ΔX^{AB} of both compounds are almost the same. In our model, δ of the cation and δ of the anion are different in Eq. (11), even though their row numbers are the same.

Therefore, the D of ZnTe and CdSe become different and the origin of the E_0 difference can be explained. If δ of the cation is the same as δ of the anion^{2,3} when their row numbers are the same, the origin of the difference of D value between CdSe and ZnTe cannot be explained.

IV. BOWING PARAMETER

E_0 of a ternary alloy $A_xB_{1-x}C$ is expressed by

$$E_0(A_xB_{1-x}C) = xE_0^{AC} + (1-x)E_0^{BC} - c^{ABC}x(1-x), \quad (12)$$

where c^{ABC} is the bowing parameter of ternary alloy $A_xB_{1-x}C$. In this section we discuss the origin of the bowing parameter. The intrinsic bowing parameter can be obtained using Van Vechten's method.⁴ From the lattice constant, D , and the electronegativity difference, which are obtained using Vegard's law, $E'_0(A_xB_{1-x}C)$ is calculated using Eq. (6). The intrinsic bowing parameter c_i^{ABC} is calculated using

$$c_i^{ABC}x(1-x) = [xE_0^{AC} + (1-x)E_0^{BC}] - E'_0(A_xB_{1-x}C). \quad (13)$$

Although Van Vechten proposed that the extrinsic bowing parameter c_e^{ABC} is a function of the difference between the heteropolar band-gap energy of AC and that of BC , we propose that c_e^{ABC} depends on both the heteropolar band-gap energy and the homopolar band-gap energy. The following equation provides the extrinsic bowing parameter due to the effect of aperiodicity:

$$c_e^{ABC} = (C_0^{A-B} + E_{h_0}^{A-B})^2/W, \quad (14)$$

where C_0^{A-B} ($E_{h_0}^{A-B}$) is the difference between C_0^{AC} and C_0^{BC} ($E_{h_0}^{AC}$ and $E_{h_0}^{BC}$) and W is a bandwidth. The bowing parameter is expressed by

$$c^{ABC} = c_i^{ABC} + c_e^{ABC}. \quad (15)$$

The bowing parameters are calculated to be $c^{\text{ZnSSe}}=0.7$ and $c^{\text{ZnMgSe}}=0.1$ eV from these equations and $W=1$ eV.⁴ This result shows that these calculated bowing parameters are the same as the experimental values. We found that the bowing parameter increases when the potential fluctuation expressed by the sum of C_0^{A-B} , which is determined by the electronegativity, and $E_{h_0}^{A-B}$, which is determined by the lattice constant, increases. If we use Van Vechten's method of calculation, the calculated results are different from the experimental results of Mg-contained compounds.

V. EXPERIMENTAL PROCEDURE

To obtain the experimental value, epitaxial layers of II-VI compound semiconductors with various compositions were grown on GaAs(100) by molecular-beam epitaxy. The growth temperature was 275 °C and the source materials used were Zn, Se, Mg, and ZnS. The lattice constant perpendicular to the GaAs(100) surface (a_{\perp}) was measured by double-crystal x-ray diffraction (XRD) using (400) reflection. The lattice mismatch $\Delta a_{\perp}/a_{\text{GaAs}}$ was expressed by

$$\Delta a_{\perp}/a_{\text{GaAs}} = (a_{\perp} - a_{\text{GaAs}})/a_{\text{GaAs}} \times 100 (\%), \quad (16)$$

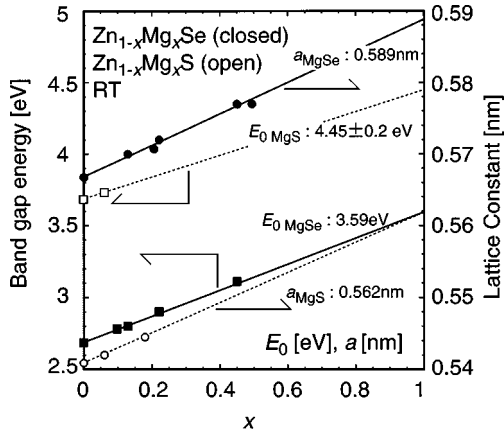


FIG. 1. Relation between the composition of Mg (x) and E_0 at RT and the lattice constant of the ternary alloys. The measured E_0 of MgS and MgSe is 4.45 ± 0.2 and 3.59 eV, respectively, and the measured lattice constant a of MgS and MgSe is 0.562 and 0.589 nm, respectively.

where a_{GaAs} is the lattice constant of GaAs, 0.5653 nm. Some samples were measured using (224) reflection to determine both a_{\perp} and the lattice constant parallel to the GaAs(100) surface (a_{\parallel}). Photoluminescence (PL) measurements were carried out at RT and 77 K. The samples were excited by a He-Cd laser with an excitation energy of 10 mW. We regard the energy of the band-edge emission at RT as E_0 because the origin of band-edge emission at RT is considered to be a band-to-band transition at Γ . The compositions of ternary and quaternary alloys were determined by electron-probe microanalysis (EPMA). EPMA measurements were calibrated using chemical analysis. We used samples whose thicknesses were between 1.3 and 1.8 μm .

VI. TERNARY ALLOYS $\text{Zn}_{1-x}\text{Mg}_x\text{Se}$, $\text{Zn}_{1-x}\text{Mg}_x\text{S}$, AND $\text{ZnS}_y\text{Se}_{1-y}$

The first experiment was the growth of the ternary alloys and the measurement of the band parameters. From these measurements, we determined E_0 of MgSe and MgS at RT and the bowing parameter of $\text{Zn}_{1-x}\text{Mg}_x\text{Se}$ and $\text{ZnS}_y\text{Se}_{1-y}$. From XRD measurements, the crystal structures of all samples were found to be zincblende and all samples except $\text{ZnS}_{0.24}\text{Se}_{0.76}$ were found to be fully relaxed because the measured a_{\perp} is almost the same as a_{\parallel} . Therefore, the band parameters of these samples can be regarded as the values of the bulk crystal of zinc-blende structure. Figure 1 shows the relationship between the mole fraction of Mg (x) and E_0 of the ternary alloys at RT. From extrapolation of these experimental values, E_0 of zinc-blende MgS and MgSe were obtained as 4.45 and 3.59 eV, respectively, although E_0 of MgS has an error of about 0.2 eV because only two samples could be measured. These E_0 of MgS and MgSe are almost the same as the values estimated using the modified dielectric theory shown in Table II and are consistent with the tendency of the band lineup of II-VI compounds derived from Harrison's tight-binding theory.¹⁹ In this experiment, we did not grow binary compounds of MgS and MgSe because the crystal structures of binary MgS and MgSe are wurtzite or rocksalt¹⁰ and because the crystal structure of binary MgS and MgSe grown on a GaAs substrate may not be zinc

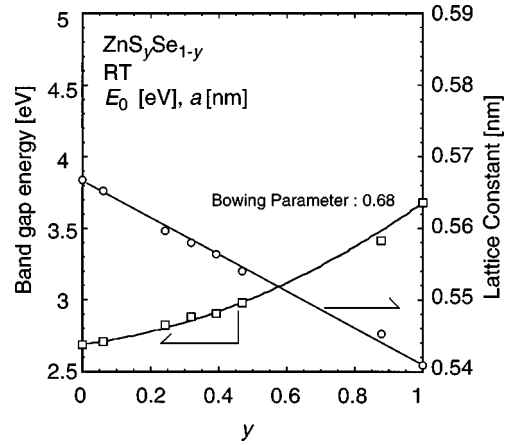


FIG. 2. Relation between the composition and E_0 of $\text{ZnS}_y\text{Se}_{1-y}$ at RT. The measured E_0 of ZnS and ZnSe is 3.68 and 2.69 eV, respectively. The bowing parameter is 0.68 eV. The fitted curve is drawn using the least-squares method.

blende. The bowing parameters of E_0 of $\text{Zn}_{1-x}\text{Mg}_x\text{Se}$ obtained is 0 eV, as can be seen in Fig. 1. This value is quite close to the calculated value 0.1 eV in Eq. (15). Although we cannot determine the bowing parameter of $\text{Zn}_{1-x}\text{Mg}_x\text{S}$ from Fig. 1, we can assume it to be 0 eV because Asano *et al.* observed the small bowing parameter of a similar alloy $\text{Zn}_{1-x}\text{Mg}_x\text{Te}$.²⁰ Figure 1 also shows the relation between the mole fraction of Mg and the lattice constant. By extrapolation of the lattice constant of $\text{Zn}_{1-x}\text{Mg}_x\text{Se}$ and $\text{Zn}_{1-x}\text{Mg}_x\text{S}$, the lattice constants of zinc-blende MgS and MgSe are 0.562 and 0.589 nm, respectively. These experimental lattice constants are almost the same as the calculated lattice constants in Table II.

Figure 2 shows the relationship between the mole fraction of S (y) and E_0 at RT, which was obtained by PL measurements, and the lattice constant of $\text{ZnS}_y\text{Se}_{1-y}$. The E_0 of ZnSe and ZnS were 2.69 and 3.68 eV, respectively and the bowing parameter of $\text{ZnS}_y\text{Se}_{1-y}$ was found to be 0.68 eV by using the least-squares method. This value is almost the same as the value calculated using Eq. (15). This value is almost the same as that measured by Ebina, Fukunaga, and Takahashi.²¹ We confirmed that the lattice constant of $\text{ZnS}_y\text{Se}_{1-y}$ can be expressed by Vegard's law.

VII. QUATERNARY ALLOY $\text{Zn}_{1-x}\text{Mg}_x\text{S}_y\text{Se}_{1-y}$

In this section we discuss the lattice constant and E_0 of the $\text{Zn}_{1-x}\text{Mg}_x\text{S}_y\text{Se}_{1-y}$ alloy. Figure 3 shows the composition dependence of the contour curves of the experimental $\Delta a_{\perp}/a_{\text{GaAs}}$ and E_0 at RT. In Fig. 3 the compositions of the samples are expressed by the open squares and the contour curves are drawn based on the experimental $\Delta a_{\perp}/a_{\text{GaAs}}$ and E_0 of these samples using interpolation and extrapolation. We used $\Delta a_{\perp}/a_{\text{GaAs}}$ in Fig. 3 because we cannot calculate the lattice constant of the bulk crystal because the elastic constant of the alloy is not known. From the XRD measurement, the crystal structure of all samples was found to be zinc blende and that of MgS and MgSe can be regarded as zinc blende when these compounds are incorporated in a $\text{Zn}_{1-x}\text{Mg}_x\text{S}_y\text{Se}_{1-y}$ alloy. The lattice constant of samples denoted by the shaded square was measured using (224) reflec-

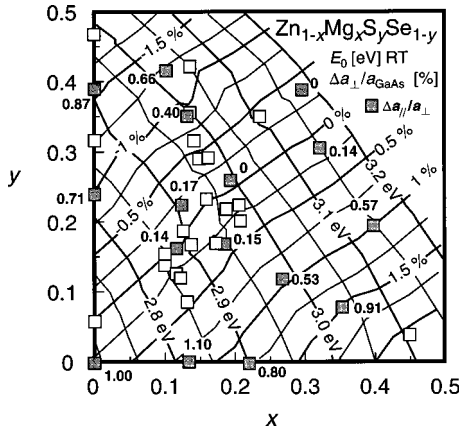


FIG. 3. Experimental data of lattice mismatch ($\Delta a_{\perp}/a_{\text{GaAs}}$) and E_0 of $\text{Zn}_{1-x}\text{Mg}_x\text{S}_y\text{Se}_{1-y}$ at RT. The contour curves are drawn based on the experimental $\Delta a_{\perp}/a_{\text{GaAs}}$ and E_0 of these samples using interpolation and extrapolation. Samples denoted by shaded squares were measured using XRD using (224) reflection to determine $\Delta a_{\parallel}/\Delta a_{\perp}$. $\Delta a_{\parallel}/\Delta a_{\perp}$ is expressed in bold characters.

tion peaks to determine $\Delta a_{\parallel}/\Delta a_{\perp}$, where $\Delta a_{\parallel} = a_{\parallel} - a_{\text{GaAs}}$ and $\Delta a_{\perp} = a_{\perp} - a_{\text{GaAs}}$. In this paper we hold that $\Delta a_{\parallel}/\Delta a_{\perp} > 0.7$ indicates that the epitaxial layer is fully relaxed and that $\Delta a_{\parallel}/\Delta a_{\perp} < 0.2$ indicates that the epitaxial layer has grown coherently.

If Mg atoms exist at interstitial sites of the crystal due to high ionicity, the contour curve for the lattice mismatch would not be linear. In Fig. 3 the contour curve that expresses the composition of $\text{Zn}_{1-x}\text{Mg}_x\text{S}_y\text{Se}_{1-y}$ lattice matched to GaAs is almost linear. This result shows that Vegard's law holds well for the lattice constant. Therefore, it can be considered that Mg atoms exist at the host lattice of zinc-blende $\text{Zn}_{1-x}\text{Mg}_x\text{S}_y\text{Se}_{1-y}$ even if the crystal structure of binary MgS and MgSe is rocksalt or wurtzite.

From the measured $\Delta a_{\parallel}/\Delta a_{\perp}$ in Fig. 3, the $\text{Zn}_{1-x}\text{Mg}_x\text{S}_y\text{Se}_{1-y}$ quaternary layers are grown coherently when $-0.5\% < \Delta a_{\perp}/a_{\text{GaAs}} < 0.5\%$. Even when $x=0.30$ and $y=0.39$, $\Delta a_{\parallel}/\Delta a_{\perp} = 0$. $\text{Zn}_{1-x}\text{Mg}_x\text{S}_y\text{Se}_{1-y}$ can be grown coherently as zinc blende, although the mole fraction of Mg is relatively high. Even though $\Delta a_{\perp}/a_{\text{GaAs}} < 0.5\%$, the binary compound ZnSe, whose $\Delta a_{\perp}/a_{\text{GaAs}}$ is 0.27%, is fully relaxed. This result shows that the critical thickness of the quaternary alloy is larger than that of the binary compounds. Other experimental results with ZnSe and $\text{ZnS}_y\text{Se}_{1-y}$ (Ref. 22) are similar. When $\Delta a_{\perp}/a_{\text{GaAs}} = +1\%$ and -1% , the $\text{Zn}_{1-x}\text{Mg}_x\text{S}_y\text{Se}_{1-y}$ quaternary layer is partially relaxed and when $\Delta a_{\perp}/a_{\text{GaAs}} < -1.5\%$ and $\Delta a_{\perp}/a_{\text{GaAs}} > 1.5\%$, $\text{Zn}_{1-x}\text{Mg}_x\text{S}_y\text{Se}_{1-y}$ is fully relaxed. The ternary alloy $\text{ZnS}_y\text{Se}_{1-y}$ is fully relaxed at $\Delta a_{\perp}/a_{\text{GaAs}} = -1\%$ and $\text{Zn}_{1-x}\text{Mg}_x\text{Se}$ is fully relaxed when $\Delta a_{\perp}/a_{\text{GaAs}} = 0.7\%$.

In the region where $x < 0.5$ and $y < 0.5$ in Fig. 3, there are many kinks in the contour curves. Some kinks are due to a fluctuation about 10–20 meV of E_0 by the stress in the samples. Some samples are coherently grown and some samples are partially relaxed due to differences in the growth conditions. Variations of the alloy composition in the whole epitaxial layer may exist due to imperfect controllability of the flux intensity and the substrate temperature. There are no large kinks due to discontinuity, which indicates a miscibility

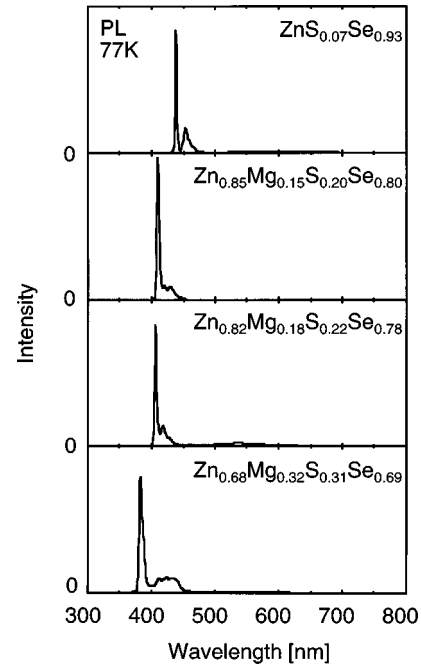


FIG. 4. 77-K photoluminescence (PL) spectrum of undoped samples.

gap and/or that the crystal structure is different.

Figure 4 shows 77-K PL spectra of undoped $\text{ZnS}_{0.07}\text{Se}_{0.93}$, $\text{Zn}_{0.85}\text{Mg}_{0.15}\text{S}_{0.20}\text{Se}_{0.80}$, $\text{Zn}_{0.82}\text{Mg}_{0.18}\text{S}_{0.22}\text{Se}_{0.78}$, and $\text{Zn}_{0.68}\text{Mg}_{0.32}\text{S}_{0.31}\text{Se}_{0.69}$, which are almost lattice matched to GaAs. The band-edge emission, which is the emission due to the donor-bound exciton or free exciton, is dominant and the intensity of the deep emission is very weak. The peak observed in the lower-energy side of the band-edge emission originates from the impurity of the sources. Extraordinary broadening of the band-edge emission, which indicates phase separation, was not observed at 77 K and RT.

E_0 and the lattice constant a of the quaternary alloy $\text{Zn}_{1-x}\text{Mg}_x\text{S}_y\text{Se}_{1-y}$ are expressed by the parabolic function^{6,11,12}

$$E_0(x, y) = xyE_0^{\text{MgS}} + (1-x)yE_0^{\text{ZnS}} + x(1-y)E_0^{\text{MgSe}} + (1-x) \times (1-y)E_0^{\text{ZnSe}} - x(1-x)\{yc^{\text{ZnMgS}} + (1-y) \times c^{\text{ZnMgSe}}\} - y(1-y)\{xc^{\text{MgSSe}} + (1-x)c^{\text{ZnSSe}}\}, \quad (17)$$

$$a(x, y) = xy a^{\text{MgS}} + (1-x)y a^{\text{ZnS}} + x(1-y) a^{\text{MgSe}} + (1-x)(1-y) a^{\text{ZnSe}}. \quad (18)$$

Because the cations mixed in are the same, we assume the equation

$$c^{\text{ZnMgS}} = c^{\text{ZnMgSe}} \quad (19)$$

and because the anions mixed in are the same, we assume the equation

$$c^{\text{MgSSe}} = c^{\text{ZnSSe}}, \quad (20)$$

E_0 and the lattice constant a of the $\text{Zn}_{1-x}\text{Mg}_x\text{S}_y\text{Se}_{1-y}$ quaternary alloy were calculated using Eqs. (17)–(20). The cal-

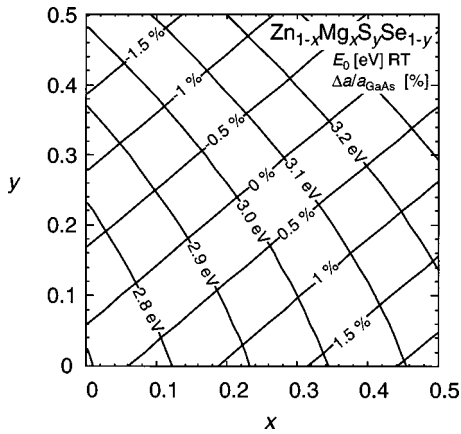


FIG. 5. Calculated value of the lattice mismatch ($\Delta a/a_{\text{GaAs}}$) and E_0 at RT. The calculated values were obtained using Eqs. (17)–(20). The parameters used are as follows. E_0 of ZnSe, ZnS, MgSe, and MgS is 2.69, 3.68, 3.59, and 4.65 eV, respectively. The bowing parameter of $\text{ZnS}_y\text{Se}_{1-y}$ and $\text{MgS}_y\text{Se}_{1-y}$ is 0.68 eV and that of $\text{Zn}_{1-x}\text{Mg}_x\text{S}$ and $\text{Zn}_{1-x}\text{Mg}_x\text{Se}$ is 0 eV. The lattice constants of ZnSe, ZnS, MgSe, and MgS are 0.5668, 0.5409, 0.589, and 0.562 nm, respectively.

culated contour curves of E_0 and the lattice constant a are shown in Fig. 5. We adjusted the E_0 value of MgS to the experimental value in Fig. 3 within the range of error of E_0 of MgS in Fig. 1. The calculated contour curves (E_0 and $\Delta a/a_{\text{GaAs}}$) in Fig. 5 overlapped the experimental contour

curves in Fig. 3 when we use E_0 of MgS of 4.65 eV. Although the contour curves in Fig. 3 are drawn referring to the measured $\Delta a_{\perp}/a_{\text{GaAs}}$, Fig. 5 shows the contour curves of the lattice mismatch of the bulk parameter $\Delta a/a_{\text{GaAs}}$.

VIII. CONCLUSION

The E_0 of MgSe and MgS at room temperature were experimentally obtained as 3.59 and 4.45 ± 0.2 eV, respectively. E_0 of various compound semiconductors was calculated using a modified dielectric theory. The experimental E_0 of MgS and MgSe are almost the same as the calculated values. The bowing parameter of the $\text{Zn}_{1-x}\text{Mg}_x\text{Se}$ ternary alloy is nearly 0 eV. This value can be explained in terms of our modified dielectric theory. The lattice constant of the quaternary alloy $\text{Zn}_{1-x}\text{Mg}_x\text{S}_y\text{Se}_{1-y}$ can be expressed by Vegard's law. E_0 of $\text{Zn}_{1-x}\text{Mg}_x\text{S}_y\text{Se}_{1-y}$ can be expressed by the parabolic function of the composition including the bowing parameter, when we use 4.65, 3.59, 3.68, and 2.69 eV as E_0 of MgS, MgSe, ZnS, and ZnSe, respectively.

ACKNOWLEDGMENTS

We would like to thank S. Itoh, K. Nakano, M. Ozawa, F. Hiei, S. Taniguchi, H. Yoshida, T. Kawasumi, and S. Kijima for fruitful discussions, Y. Morioka for her EPMA measurements, and Professor K. Akimoto, Dr. T. Miyajima, Dr. M. Ikeda, Dr. Y. Mori, Dr. J. Seto, and Dr. T. Yamada for their encouragement during the course of this work.

- ¹J. C. Phillips, Phys. Rev. **112**, 685 (1958).
- ²J. A. Van Vechten, Phys. Rev. **182**, 891 (1969).
- ³J. A. Van Vechten, Phys. Rev. **187**, 1007 (1969).
- ⁴J. A. Van Vechten and T. K. Bergstresser, Phys. Rev. B **1**, 3351 (1970).
- ⁵G. B. Stringfellow, J. Electron. Mater. **10**, 919 (1981).
- ⁶S. Taniguchi, T. Hino, S. Itoh, N. Nakayama, A. Ishibashi, and M. Ikeda, Electron. Lett. **32**, 552 (1996).
- ⁷H. Okuyama, K. Nakano, T. Miyajima, and K. Akimoto, Jpn. J. Appl. Phys., Part 2 **30**, L1620 (1991).
- ⁸H. Okuyama, N. Nakayama, S. Itoh, M. Ikeda, and A. Ishibashi, Jpn. J. Appl. Phys., Part 1 **35**, 1410 (1996).
- ⁹N. Nakayama, S. Itoh, T. Ohata, K. Nakano, H. Okuyama, M. Ozawa, A. Ishibashi, M. Ikeda, and Y. Mori, Electron. Lett. **29**, 1488 (1993).
- ¹⁰H. Mittendorf, Z. Phys. **183**, 113 (1965).
- ¹¹S. Adachi, J. Appl. Phys. **53**, 875 (1982).
- ¹²C. K. Williams, T. H. Glisson, J. R. Hauser, and M. A. Littlejohn, J. Electron. Mater. **7**, 639 (1978).
- ¹³L. Pauling, *The Nature of the Chemical Bond* (Cornell University Press, Ithaca, 1960).
- ¹⁴L. Vegard, Z. Phys. **5**, 17 (1921).
- ¹⁵R. S. Mulliken, J. Chem. Phys. **2**, 782 (1934); **3**, 573 (1935).
- ¹⁶S. G. Lias, J. E. Bartmess, J. L. Holmes, R. D. Levin, J. F. Liebman, and W. G. Mallard, J. Phys. Chem. Ref. Data **17**, 861 (1988).
- ¹⁷H. Hotop and W. C. Lineberger, J. Phys. Chem. Ref. Data **14**, 731 (1985).
- ¹⁸C. Nording, Ark. Fys. **15**, 397 (1959).
- ¹⁹W. A. Harrison, *Electronic Structure and the Properties of Solids* (Dover, New York, 1989).
- ²⁰T. Asano, K. Funato, F. Nakamura, and A. Ishibashi, J. Cryst. Growth **156**, 373 (1995).
- ²¹A. Ebina, E. Fukunaga, and T. Takahashi, Phys. Rev. B **10**, 2495 (1974).
- ²²Sz. Fujita, K. Terada, T. Sakamoto, and Sg. Fujita, J. Cryst. Growth **94**, 102 (1989).
- ²³W. B. Pearson, *Crystal Chemistry and Physics of Metals and Alloys* (Wiley, New York, 1972).
- ²⁴S. M. Sze, *Physics of Semiconductor Devices* (Wiley, New York, 1981).
- ²⁵H. C. Casey, Jr. and M. B. Panish, *Heterostructure Lasers* (Academic, New York, 1978).